

Computer Simulation and Noise Analysis of the System Performance of 1.55- μm Single-Frequency Semiconductor Lasers

TEK-MING SHEN, MEMBER, IEEE, AND GOVIND P. AGRAWAL, SENIOR MEMBER, IEEE

Abstract—A theoretical model for the noise analysis of the system performance of 1.55- μm single-frequency semiconductor lasers is presented. Computer simulations are used to analyze the role of various noise sources in a 1.7-Gbit/s transmission experiment where the data was transmitted over 69 km using a 1.56- μm distributed-feedback laser. The bit-error-rate curves generated from numerical simulations agree well with the results of the transmission experiment. The relative contributions of various noise sources in limiting the system performance are discussed and compared. In particular, we consider circuit noise, shot noise, laser intensity noise, mode-partition noise, parasitic reflections, and the frequency chirp.

I. INTRODUCTION

RECENTLY much effort has been concentrated on studying lightwave transmission at 1.55 μm using single-frequency lasers [1]–[9]. The performance of these transmission experiments depends critically on various noise sources such as mode-partition noise, the frequency chirp, reflection-induced noise, shot noise, and circuit noise of the front-end amplifiers used in receivers. In some of the transmission experiments, a noise floor in the bit-error-rate curve was observed [1], [2] and attributed to mode-partition noise. In other experiments, lasers with extremely high side-mode suppression ratio (> 1000) were used [3], [7] and in most of these experiments [5], [6] the transmission distance was found to be limited by the chirp. Recent experiments, using a single-frequency laser with low chirp (0.4 Å) and low-loss fibers (0.20 dB/km), have achieved repeaterless transmission distance of 130 km at 2 Gbit/s [8] and 103 km at 4 Gbit/s [9]. Meanwhile, another report has suggested that reflection-induced noise [10] can play an important role in governing the performance of lightwave systems.

In this paper we provide a theoretical basis for the simulation of bit-error-rate curves in transmission experiments. Computer simulations are used to analyze the relative contribution of each noise source to the measured bit error rate, and hence provide an indication of the direction through which the system performance can be improved. Such an analysis would be difficult to carry out experimentally because it is difficult to separate the con-

tribution of each noise source. We use computer simulations to analyze the system performance of a transmission experiment where the data was transmitted at 1.7 Gbit/s over 69 km of single-mode fiber using a 1.56- μm distributed-feedback double-channel planar-buried-heterostructure (DFB-DCPBH) laser [11], [12]. Our results suggest that in this transmission experiment the system suffered severe performance degradation from parasitic reflections and chirp. Parasitic reflections degrade the receiver sensitivity while the chirp limits the transmission distance because of dispersion-induced delay of various frequency components. Our results also show that mode-partition noise is not a major source of error in our case as there are only two side modes and the side-mode suppression ratio is greater than 1000. This conclusion is consistent with the theoretical calculation based on photon statistics [13], [14] as well as with other transmission experiments [8], [15].

In the following sections, we first present the results of a transmission experiment performed using a 1.56- μm DFB-DCPBH laser. We then discuss the theoretical framework which is used to simulate the results of the transmission experiment. Finally we discuss the limitation on the bit-rate-distance product set by each noise source.

II. 1.7-GBIT/S TRANSMISSION EXPERIMENT

We have performed a transmission experiment at 1.7 Gbit/s using a 1.56- μm DFB-DCPBH single-frequency laser. This laser has a second-order grating etched on the substrate and has no antireflection coatings on its facets. It shows single-mode operation up to the 3-mW level with a mode suppression ratio of 1000 to 1 under both dc and 1.7-Gbit/s modulation. The transmission experiment was performed at 1.7 Gbit/s with a pseudorandom NRZ bit pattern over a distance of 69 km of single-mode fiber with an average loss of 0.25 dB/km and a dispersion of 17 ps/km-nm. The receiver used has a high impedance GaAs FET preamplifier with a SAGM APD [3], [16]. The power coupled into the fiber was -4.6 dBm. The off: on extinction ratio was 1:6. This laser was particularly sensitive to parasitic reflections and showed ~ 10 percent amplitude variation in the optical spectrum which was monitored simultaneously during the transmission experiment.

Manuscript received July 18, 1986; revised September 25, 1986.
The authors are with AT&T Bell Laboratories, Murray Hill, NJ 07974.
IEEE Log Number 8612220.

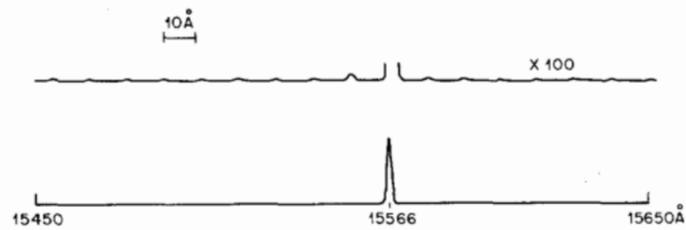


Fig. 1. Longitudinal-mode spectrum of the DFB-DCPBH laser under 1.7-Gbit/s modulation. The mode suppression ratio is 1000 to 1.

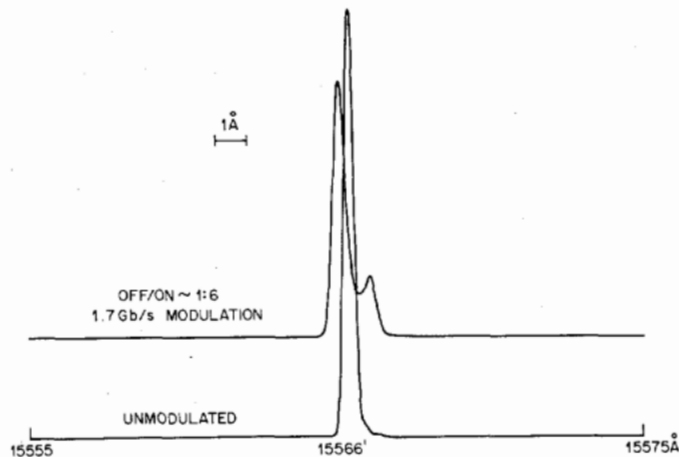


Fig. 2. Chirp-induced line broadening of the DFB-DCPBH laser under 1.7-Gbit/s modulation. The chirp amplitude is about 1 Å.

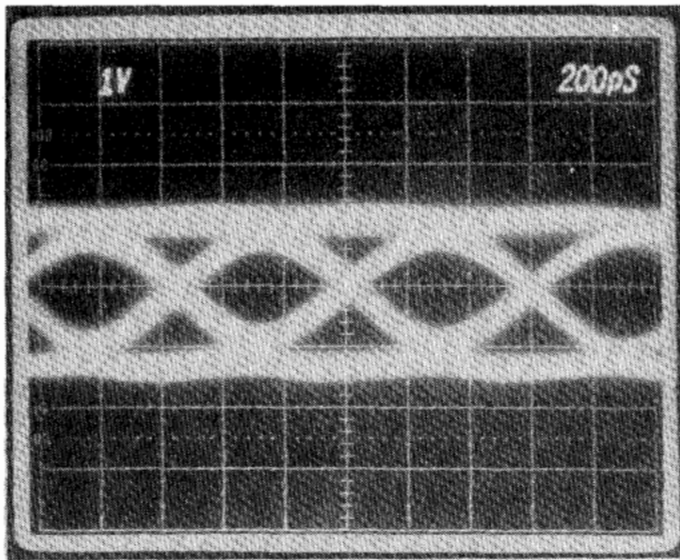


Fig. 3. Eye diagram of the received signal at 1.7 Gbit/s after transmission over 69 km of fiber.

Fig. 1 shows the optical spectrum under the above operating conditions. The mode suppression ratio of the laser under 1.7 Gbit/s modulation is 1000:1. Fig. 2 shows the chirp of about 1 Å resulting from the 1.7 Gbit/s modulation. Fig. 3 shows the received eye diagram at 1.7 Gbit/s after a transmission over 69 km. Fig. 4 shows the bit error rate curves for 3 m and 69 km of fibers. The system suffered a 2.2-dB power penalty at 1×10^{-9} bit error rate. In the following section we use computer sim-

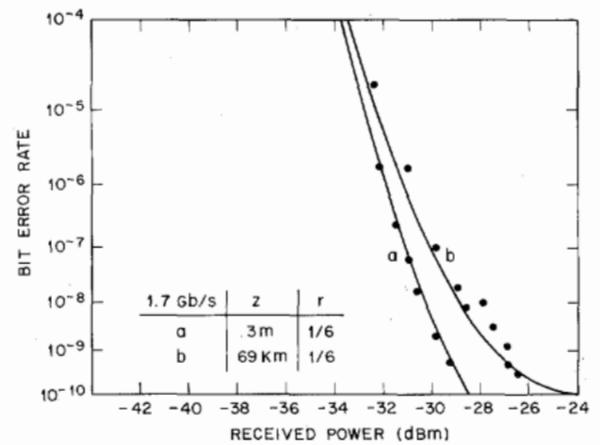


Fig. 4. Experimental data points (•) and simulated bit-error-rate curves (solid line) of the 1.7-Gbit/s transmission experiment. Fiber length is 3 m for curve *a* and 69 km for curve *b*.

ulations to analyze the contribution of each noise source to the system performance degradation.

III. THEORY

We first present the theoretical framework used in our computer simulations. The noise sources we consider include circuit noise, shot noise, laser intensity noise, reflection-induced noise, mode-partition noise, and chirp-induced noise. The circuit noise and the shot noise govern the ultimate receiver sensitivity; their contribution does not lead to a floor in the bit-error-rate curves. The laser intensity noise and the reflection-induced noise degrade the receiver sensitivity and can lead to a bit-error-rate floor if their magnitude is large enough [10]. However, since their contribution is nondispersive, they do not impose any limitation on the transmission distance, i.e., their contribution is merely degrading the receiver sensitivity over that expected only from the circuit noise and shot noise. By contrast, the contribution of both the mode partition and the chirp depends on fiber dispersion. Their presence can therefore severely limit the transmission distance. Among the two, the chirp is expected to be the most limiting factor for the performance of single-frequency semiconductor lasers.

We consider an avalanche photodetector (APD) on which a random bit stream consisting of "1" and "0" (on and off states) is incident at the bit rate B . The detected signal S_1 or S_0 in the two states is the average current given by [17]

$$S_j = \left(\frac{\eta q}{h\nu} \right) \langle M \rangle b_j, \quad j = 0 \text{ or } 1 \quad (1)$$

where $(\eta q/h\nu)$ is the responsivity of a detector with quantum efficiency η to the incident photons of energy $h\nu$, $\langle M \rangle$ is the average APD gain, and b_j is the average power received during a single bit. The bit error rate results from the noise current σ_j associated with the signal S_j . Assuming the Gaussian statistics, the probability that a bit is incorrectly identified or the bit error rate is given by [17]

$$P(E) = \frac{1}{\sqrt{2\pi}} \int_Q^\infty \exp(-x^2/2) dx$$

$$= \frac{1}{2} \operatorname{erfc}(Q/\sqrt{2}) \quad (2)$$

where $\operatorname{erfc}(x)$ denotes the complimentary error function and

$$Q = \frac{D - S_0}{\sigma_0} = \frac{S_1 - D}{\sigma_1} \quad (3)$$

The decision level D is chosen to yield equal $P(E)$ in the two states. Eliminating D in (3) gives

$$Q = (S_1 - S_0)/(\sigma_0 + \sigma_1). \quad (4)$$

A value of $Q \geq 6$ is required to maintain $P(E)$ below 10^{-9} . Writing $r = b_0/b_1$ as the off/on extinction ratio, and $P_{\text{av}} = (b_0 + b_1)/2$ as the average detected power, (4) becomes

$$Q = \left(\frac{1-r}{1+r} \right) \left(\frac{\eta q}{h\nu} \right) \langle M \rangle \frac{2P_{\text{av}}}{(\sigma_0 + \sigma_1)}. \quad (5)$$

The noise current σ_j gets contributions from several sources. In what follows we discuss the contribution of each noise source. The analysis is applicable to both the "off" and "on" states denoted by $j = 0$ or 1 . For our transmission experiment the "off" state is above threshold. The total noise current is thus obtained by taking the root-mean-square value of the individual noise currents. The bit-error-rate curves can be generated by using (2) and (5).

A. Circuit Noise

The circuit noise is the contribution to the output noise from the amplifier and the bias circuit. For a receiver that has been incorporated with an FET front-end amplifier [3], the variance of the noise current at the bit rate B (due to the amplifier and bias resistor referred to the input) is [17]

$$\sigma_{c,j}^2 = \left[\frac{4kT}{R_L} \left(1 + \frac{\Gamma}{g_m R_L} \right) + 2qI_{\text{dk}} \right] J_2 B$$

$$+ 4kT\Gamma \frac{(2\pi C)^2}{g_m} J_3 B^3. \quad (6)$$

Here g_m is the transconductance of the FET preamplifier, C is the total input capacitance, R_L is the load resistance, and I_{dk} is the dark current. For a GaAs FET the numerical factor $\Gamma \approx 1.15$. The parameters J_2 and J_3 are the weighting factors and depend on the input and output pulse shapes [18]. Note that $\sigma_{c,j}$ is the same for both the "on" and "off" states. Equation (6) is obtained from a simplified circuit model. In our simulations we use $\sigma_{c,j}^2$ as a fitting parameter to the measured receiver sensitivity.

B. Shot Noise

The variance of the noise current due to shot noise is given by [19]

$$\sigma_{\text{sn},j}^2 = 2q \langle M \rangle F(M) S_j J_2 B. \quad (7)$$

Here $\langle M \rangle$ is the average APD gain and $F(M)$ is the excess noise factor which can be expressed as [19], [20]

$$F(M) = k \langle M \rangle + \left(2 - \frac{1}{\langle M \rangle} \right) (1 - k) \quad (8)$$

where k is the ionization ratio of the majority and minority carriers.

C. Laser Intensity Noise

The laser power in general fluctuates with variance σ_{laser}^2 . These power fluctuations induce noise in the signal current governed by

$$\sigma_{\text{sig}}^2 = \left(\frac{\eta q}{h\nu} \right)^2 \langle M \rangle^2 \sigma_{\text{laser}}^2. \quad (9)$$

Laser power fluctuations can be calculated using the rate equations [21]. It can be shown that if N_p and N_e are the number of photons and carriers in the laser cavity, the variance of N_p is approximately given by

$$\sigma_{N_p}^2 \approx \langle N_p \rangle + \langle N_e \rangle. \quad (10)$$

Typically, $\langle N_e \rangle \geq 10^8$ while $\langle N_p \rangle \sim 10^5$, implying that $\sigma_{N_p} \approx \langle N_e \rangle^{1/2}$. Note that in this model the noise power is roughly clamped at threshold and is independent of the laser power [22]. Typical values of the noise power observed experimentally are ~ -23 dBm for a 2-GHz bandwidth. For an "on" state power level of 2 mW, this corresponds to a signal-to-noise ratio (SNR) of 400. We use SNR as the model parameter and rewrite (9) as

$$\sigma_{\text{sig},j}^2 = \left(\frac{\eta q}{h\nu} \right)^2 \langle M \rangle^2 \left(\frac{b_1}{\text{SNR}} \right)^2 \quad (11)$$

both for the "on" and "off" states, since in our case the "off" state is above threshold.

D. Reflection-Induced Noise

External optical feedback into the laser cavity will cause the laser to develop side modes around the main mode. These side modes are the external cavity modes and cause additional fluctuations in the laser power. If the signal-to-noise ratio induced by reflection is $(\text{SNR})_{\text{ref}}$, the variance of noise current is [10]

$$\sigma_{\text{ref},j}^2 = \left(\frac{\eta q}{h\nu} \right)^2 \langle M \rangle^2 \frac{b_j^2}{(\text{SNR})_{\text{ref}}^2},$$

$$j = 0 \text{ or } 1. \quad (12)$$

We assume that the parameter $(\text{SNR})_{\text{ref}}$ is the same for the "on" and "off" states. This is a reasonable assumption since the effect should depend on the fractional amount of power reflected back into the laser, and in our case both the "on" and "off" states are above threshold.

E. Mode-Partition Noise

The presence of longitudinal side modes in single-frequency lasers will introduce mode partition noise in light-

wave systems [14], [15]. The noise due to side modes consists of two parts. First, the presence of side modes will cause additional fluctuations in the laser power. Second, after traveling through a dispersive fiber, the power carried by the side modes will be dispersed relative to the main mode. This causes dispersion-induced fluctuations in the received power. These two effects can be combined to give an effective mode suppression ratio [14]

$$(\text{MSR})_{\text{eff}} = \text{MSR} / \sqrt{2N} \quad (13)$$

where we assumed that there are N side modes with a constant mode-suppression ratio. It can be shown that the variance of noise current cannot be greater than

$$\sigma_{mpn,j}^2 = \left(\frac{\eta q}{h\nu} \right)^2 \langle M \rangle^2 \frac{2N b_j^2}{(\text{MSR})_{\text{eff}}^2}. \quad (14)$$

We shall conservatively use equation (14) for mode-partition noise in our simulations.

F. Chirp

Chirp of single-frequency lasers is a major source of error in high bit-rate transmission. The carrier and photon density variations result in relaxation oscillations with frequency ν_R and a damping time constant Γ . Because of these relaxation oscillations the optical pulse and the wavelength both exhibit damped transient oscillations during the turn-on and turn-off of the laser pulse. These are described by

$$p(t) = p_0 \sin(2\pi\nu_R t - \delta) e^{-\Gamma t} \quad (15)$$

$$\Delta\lambda(t) = \Delta\lambda_0 \sin(2\pi\nu_R t - \theta) e^{-\Gamma t}. \quad (16)$$

Here p_0 is the initial oscillation amplitude, $\Delta\lambda_0$ is the chirp amplitude, and δ and θ are phase angles. After traveling through a fiber with dispersion coefficient $D = (d\omega/d\lambda) \cdot (d^2\beta/d\omega^2)$ for a distance z at a bit rate B , the pulse shape will be distorted. If an undershoot of the relaxation oscillation is delayed because of fiber dispersion to appear at the decision time and falls below the decision level, an error will be detected. This pulse amplitude distortion together with the timing jitter in the decision circuit result in an amplitude noise in the receive power. The noise variation is given by (see Appendix)

$$\sigma_{ic,j}^2 = \left(\frac{\eta q}{h\nu} \right)^2 \langle M \rangle^2 \frac{p_0^2}{2} \left[\sum_{n,i} P_n^2 \exp \left[-2\Gamma \left(\frac{1}{2B} - \Delta\tau_i^n \right) \right] \right] \quad (17)$$

where $\Delta\tau_i^n$ is the solution of the transcendental equation (A3).

G. Bit-Error-Rate Curves

The various noise contributions can be added to get the total variance of the noise current

$$\sigma_j^2 = \sigma_{c,j}^2 + \sigma_{sn,j}^2 + \sigma_{sig,j}^2 + \sigma_{ref,j}^2 + \sigma_{mpn,j}^2 + \sigma_{ic,j}^2, \quad j = 0 \text{ or } 1. \quad (18)$$

Equations (2), (5), and (18) can then be used to generate the bit-error-rate curves by plotting $P(E)$ as a function of the average received power P_{av} . As an illustration of the theoretical analysis, we use it to simulate the bit-error-rate curves of the 1.7-Gbit/s transmission experiment. In the case of transmission over 3 m of fiber, there is practically no dispersion. The receiver sensitivity measured is governed by circuit noise, shot noise, laser intensity noise, and reflection-induced noise. Since the circuit noise and the reflection-induced noise are not accurately known, σ_c^2 and σ_{ref}^2 are determined by fitting the bit-error-rate curve a in Fig. 4 in the range from 10^{-4} to 10^{-10} . The values of σ_c^2 and σ_{ref}^2 are uniquely determined by fitting the measured receiver sensitivity at 10^{-10} bit-error-rate and the slope of the bit-error-rate curve. The shot noise is calculated with the following parameters [3], [23]: $\eta = 68$ percent, $\langle M \rangle = 9.1$, $k = 0.35$, and $J_2 = 0.79$. In a separate measurement the SNR for laser intensity noise is found to be 400 at the operating power of 2 mW. For the mode-partition noise we have measured $\text{MSR} = 1000$ for our laser, and we take the number of side modes $N = 2$ with a mode separation of 10 Å. The chirp contribution is calculated using (17) with the following experimentally determined parameters: $\nu_R = 4$ GHz, $\Gamma/\nu_R = 1$, and $p_0/b_1 = 0.15$. These parameters are only approximate and may vary by 20 percent. The fiber dispersion is 17 ps/km-nm.

IV. RESULTS AND DISCUSSION

The performance of a lightwave system is best characterized by generating the bit-error-rate curve as a function of the received power. One important feature of the bit-error-rate curves in a logarithmic plot is the change in slope that can result in the appearance of a noise floor. This feature is due to different functional dependence of the noise on the signal power for different noise sources. The circuit noise σ_c is independent of the signal power, the shot noise σ_{sn} is proportional to the square-root of the signal power ($\sqrt{b_j}$), and all the other signal induced noise contributions are proportional to the signal power (b_j). In other words, the signal-to-noise ratios or the Q -values are proportional to b_j , $\sqrt{b_j}$ and independent of b_j , respectively. It can be easily shown from (2) and (5) that in the logarithmic plot of bit-error-rate curves the circuit noise will give rise to a slope twice as large as the shot noise, while all the other noise sources will lead to the appearance of a noise floor if their contributions are sufficiently large. In order to get a feeling of the relative contributions of various noise sources in limiting the system performance, we use computer simulations to analyze the results of our transmission experiment.

The results of our computer simulation of the bit-error-rate curves for the 1.7-Gbit/s transmission experiment are shown in Fig. 4 together with the experimental data. The bit-error-rate curve a with 3 m of fiber was fitted to obtain σ_c and σ_{ref} , as discussed before. The circuit noise current of 469 nA and $(\text{SNR})_{\text{ref}} = 11$ provided a reasonable fit to both the receiver sensitivity and the observed slope of the

TABLE I

CONTRIBUTIONS TO THE NOISE CURRENT FROM VARIOUS NOISE SOURCES AT THE RECEIVED POWER OF -27 dBm WITH $Q = 6.1$ AND $P(E) = 6.7 \times 10^{-10}$ FOR THE TRANSMISSION EXPERIMENT AT 1.7 Gbit/s OVER 69 km OF FIBER

Noise Source	Noise current bit "1" (nA)	Noise current bit "0" (nA)
circuit noise	$\sigma_{c,1} = 469$	$\sigma_{c,0} = 469$
shot noise	$\sigma_{sn,1} = 675$	$\sigma_{sn,0} = 276$
laser intensity noise	$\sigma_{lig,1} = 66$	$\sigma_{lig,0} = 66$
reflection noise	$\sigma_{ref,1} = 2400$	$\sigma_{ref,0} = 401$
mode partition noise	$\sigma_{mpn,1} = 53$	$\sigma_{mpn,0} = 88$
chirp noise	$\sigma_{cn,1} = 719$	$\sigma_{cn,0} = 719$
Total	$\sigma_1 = 2640$	$\sigma_0 = 989$

(Shot noise, laser intensity noise, mode partition noise and chirp noise are calculated from experimentally determined parameters. Circuit noise and reflection-induced noise are determined by fitting the baseline bit-error-rate curve in the range from 10^{-4} to 10^{-10} .)

bit-error-rate curve *a*. Note that $(\text{SNR})_{\text{ref}}$ is the only parameter that can be varied to give the correct slope of the curve. The fitted value of $(\text{SNR})_{\text{ref}}$ is also consistent with amplitude fluctuations in the optical spectrum observed experimentally. The calculated curve *b* for 69 km of fiber was obtained without adjusting any parameter and is in reasonable agreement with the experimental data. The contributions to the noise current from various noise sources are shown in Table I. We can see that the system performance is severely limited by reflections which significantly degraded the receiver sensitivity. The additional noise due to chirp has limited the transmission distance to 69 km. However, in other transmission experiments [8], [9] the use of a low-chirp laser and low-loss (0.20 dB/km) fiber has allowed repeaterless transmission at 2 Gbit/s over 130 km and at 4 Gbit/s over 103 km. In the following we discuss the role of various noise sources in limiting the transmission distance as a function of the bit rate.

Calculations using practical values of the receiver parameters showed that any noise source has negligible effect on the receiver sensitivity if the signal-to-noise ratio for that noise source is greater than 200 [10]. With this in mind, we can estimate the relative contributions of various noise sources to the bit error rate. The laser noise in general is very small (≈ -23 dBm). For a 2-mW operating power, this corresponds to a signal-to-noise ratio of 400. This value is sufficiently large and causes a negligible power penalty in the receiver sensitivity. Fiber-far-end reflections can induce sufficient power fluctuations to result in large power penalties [10]. A power penalty of 2.5 dB due to reflection was experienced in our experiment. The reflection-induced noise is, however, independent of the length of fiber [10] and therefore does not impose any limitation on the transmission distance. The signal-to-noise ratio for mode partition noise in the extreme case varies roughly as $\text{MSR} / \sqrt{2N}$ [14]. If there are only 2 side modes, a $\text{MSR} \geq 400$ will impose negligible

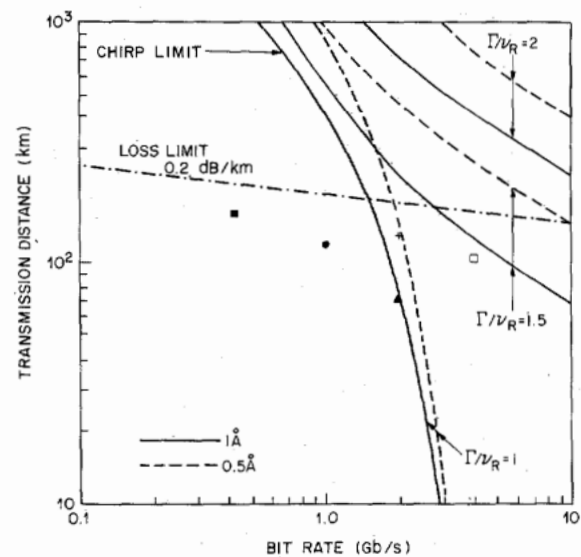


Fig. 5. Limitation on transmission distance due to fiber loss and chirp at various bit rates. Also shown are the experimental data points from [3], [5], [6], [8], [9]. Note the improvement in the chirp-limited transmission distance with an increase in the damping rate of relaxation oscillations.

power penalty in the receiver sensitivity. Since single-frequency lasers with a MSR of greater than 400 are readily available, the mode-partition noise is not expected to limit the transmission distance in single-frequency lasers. Chirp is not a limiting factor at low bit-rates, since the relaxation oscillations are sufficiently damped at the decision point. At high bit-rates (≥ 2 Gbit/s), however, the undamped relaxation oscillations would induce errors in the decision and the chirp may become the major noise source for limiting the transmission distance. In the following, we show that strong damping of relaxation oscillations is a governing factor for improving the performance of high-bit-rate long-haul lightwave systems.

Fig. 5 shows the chirp-limited transmission distance at various bit rates for a bit-error rate of 10^{-9} . Also shown is the fiber loss-limit at 0.2 dB/km assuming an average launched power of 1 mW and a receiver sensitivity of -42.6 dBm at 420 Mbit/s with an APD [3]. The chirp limits for 1 Å and 0.5 Å chirp amplitudes are calculated for lasers with relaxation damping constants $\Gamma / \nu_R = 1, 1.5$ and 2, assuming a fiber dispersion of 17 ps/km-nm. The chirp limit depends strongly on the relaxation damping constant. Also shown in Fig. 5 are the experimental points for transmission experiments at 0.42, 1, 2, and 4 Gbit/s reported in [3], [5], [6], [8], [9]. It can be seen that the transmission distances at 0.42 and 1 Gbit/s [3], [5] were loss limited, while the transmission distance at 2 Gbit/s [6] was limited by the chirp. In the other experiment at 2 Gbit/s [8] the use of a low chirp (0.4 Å) laser and low-loss (0.2 dB/km) fiber has resulted in a transmission distance of 130 km. In this experiment the transmission distance is actually loss limited due to a low launched power (-3.8 dBm) and the fiber splicing loss unaccounted for in our calculation. Operation of this laser at a higher power (-1.6 dBm) increased the damping rate

of relaxation oscillations and made it possible to perform the experiment at 4 Gbit/s over 103 km of fiber [9].

V. CONCLUSION

We have used computer simulations to analyze the system performance of a 1.7 Gbit/s transmission experiment performed using a 1.56- μm DFB-DCPBH single-frequency laser. It is demonstrated that computer simulations are very useful in analyzing the relative contribution of various noise sources to the bit-error rate. Our results show that parasitic reflections and the frequency chirp were the major noise sources in our 1.7-Gbit/s transmission experiment. We have used our numerical model to study the dispersion-limited transmission distance for lightwave systems operating in the Gbit/s range. The mode-partition noise is not a limiting factor if the single-frequency laser has its side modes suppressed by a factor of 400 or more. By contrast, the frequency chirp severely limits the system performance at high bit rates. The chirp-limited transmission distance is found to improve significantly with an increase in the damping rate Γ of relaxation oscillations. Since Γ can be increased by increasing the bias level of the laser, it may become necessary to operate the high-bit-rate lightwave systems with a relatively low extinction ratio in order to reduce the chirp and increase the transmission distance.

APPENDIX DERIVATION OF (17)

To calculate the signal-to-noise-ratio degradation induced by chirp, we consider signal transmission at the bit rate B with a time slot $T_b = 1/B$. When such a signal is transmitted through a fiber with dispersion $D = (d\omega/d\lambda) \cdot (d^2\beta/d\omega^2)$ for a distance z , the whole bit stream is delayed on average by a time $Dz\lambda_c$, where λ_c is the center wavelength. In addition, the signal at time t suffers a differential delay $\Delta\tau$ with reference to the center wavelength, where

$$\Delta\tau = Dz\Delta\lambda(t). \quad (\text{A1})$$

As a result, the decision circuit at the receiver with the decision point set at the time $T_b/2$ (with reference to the onset of a pulse) receives a signal originated at the time $T_b/2 - \Delta\tau$, where $\Delta\tau$ is given by

$$\Delta\tau = Dz\Delta\lambda(t = T_b/2 - \Delta\tau). \quad (\text{A2})$$

The effect of the differential delay $\Delta\tau$ represented by (A2) is that an undershoot in the optical pulse due to relaxation oscillations is delayed and appears at a different position of the pulse when it arrives at the decision circuit. If this undershoot happens to appear at the center of the pulse where the decision time is set and falls below the decision level, an error will occur. Equation (A2) may have multiple solutions representing different portions of the optical pulse being delayed and detected by the decision circuit. In order to account for delays $\Delta\tau$ greater than $T_b/2$, i.e., signals originating from earlier bits, we write $\Delta\tau = nT_b + \Delta\tau_i^n$ where n is an integer and $\Delta\tau_i^n$ lies be-

tween $-T_b/2$ to $+T_b/2$. Equation (A2) is then modified to become

$$nT_b + \Delta\tau_i^n = Dz\Delta\lambda(t = T_b/2 - \Delta\tau_i^n). \quad (\text{A3})$$

Each detected signal presents a fluctuation of magnitude $p(t = T_b/2 - \Delta\tau_i^n)$ about the mean value b_1 of the bit "1". Let P_n be the probability of finding a bit "1" in the n th bit. The total fluctuation about the mean value b_1 of the bit "1" at the decision point is then given by

$$\Delta = \sum_{n,i} P_n \cdot p(t = T_b/2 - \Delta\tau_i^n). \quad (\text{A4})$$

For $n = 0$, i.e., for the bit under consideration, $P_n = 1$. For other bits $n \neq 0$, $P_n = \frac{1}{2}$ for a pseudorandom sequence since there are equal probabilities for other bits to be "1" or "0". Equation (A4) is a conservative estimate because it assumes that every bit of "1" starts with a relaxation oscillation that is not generally the case in the non-return-to-zero format of the pseudorandom word modulation.

We assume that there exists significant time jitter in the decision time and average the fluctuation Δ over one relaxation-oscillation cycle. This is a fair assumption since under normal operating conditions the relaxation-oscillation frequency is about 4–5 GHz which corresponds to a time scale of 200–250 ps, a reasonable value of time jitter. Using (15) in (A4) and performing the average, we obtain

$$\langle \Delta \rangle = 0 \quad (\text{A5})$$

and

$$\langle \Delta^2 \rangle = \sum_{n,i} P_n^2 \cdot \frac{P_0^2}{2} \exp[-2\Gamma(T_b/2 - \Delta\tau_i^n)]. \quad (\text{A6})$$

The standard deviation of the amplitude fluctuation is

$$\begin{aligned} \sigma &= \sqrt{\langle \Delta^2 \rangle - \langle \Delta \rangle^2} \\ &= \frac{P_0}{\sqrt{2}} \left[\sum_{n,i} P_n^2 \exp[-2\Gamma(T_b/2 - \Delta\tau_i^n)] \right]^{1/2}. \quad (\text{A7}) \end{aligned}$$

The standard deviation of the photocurrent fluctuation is obtained by multiplying σ by $(\eta q/h\nu) \langle M \rangle$. This leads to (17) of the text if we replace T_b by $1/B$.

ACKNOWLEDGMENT

The authors wish to thank R. A. Linke and B. L. Kasper for performing the 1.7-Gbit/s transmission experiment.

REFERENCES

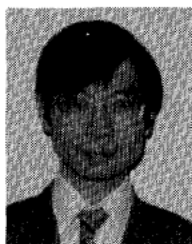
- [1] R. A. Linke, B. L. Kasper, J. S. Ko, I. P. Kaminow, and R. S. Vodhanel, "A 1 Gbit/s transmission experiment over 101 km of single mode fiber using a 1.55 μm ridge guide C³ laser," *Electron. Lett.*, vol. 19, pp. 775–776, 1983.
- [2] H. Nishimoto, H. Kuwahara, and M. Motegi, "Injection-locked 1.5- μm InGaAsP/InP lasers capable of 450 Mbit/s transmission over 106 km," *Electron. Lett.*, vol. 19, pp. 509–510, July 1983.
- [3] B. L. Kasper, R. A. Linke, J. C. Campbell, A. G. Dentai, R. S. Vodhanel, P. S. Henry, I. P. Kaminow, and J-S Ko, "A 161.5- μm transmission experiment at 420 Mbit/s," presented at ECOC, Geneva, Switzerland, Oct. 1983.

- [4] H. Toba, Y. Kobayashi, and K. Yanagimoto, "Injection-locking technique applied to a 170-km transmission experiment at 445.8 Mbit/s," *Electron. Lett.*, vol. 20, pp. 370-371, Apr. 1984.
- [5] R. A. Linke, B. L. Kasper, J. C. Campbell, A. G. Dentai, and I. P. Kaminow, "120-km lightwave transmission experiment at 1 Gbit/s using a new long-wavelength avalanche photodetector," *Electron. Lett.*, vol. 20, pp. 498-449, June 1984.
- [6] R. A. Linke, B. L. Kasper, R. M. Jopson, J. C. Campbell, A. G. Dentai, W. T. Tsang, N. A. Olsson, R. A. Logan, L. S. Johnson, and C. H. Henry, "A 2-Gbit/s 71-km transmission experiment using a 1.5- μm ridge-type distributed feedback (DFB) laser," presented at IOOC, Tokyo, Japan, 1983.
- [7] P. J. Chidgey, B. R. White, M. C. Brain, R. C. Hooper, D. R. Smith, P. P. Smyth, P. J. Fiddymant, A. W. Nelson, and L. D. Westbrook, "1.2-Gbit/s optical fiber transmission experiment over 113.7 km using a 1.528- μm distributed-feedback ridge-waveguide laser," *Electron. Lett.*, vol. 20, pp. 707-709, Aug. 1984.
- [8] B. L. Kasper, R. A. Linke, K. L. Walker, L. G. Cohen, T. L. Koch, T. J. Bridges, E. G. Burkhardt, R. A. Logan, R. W. Dawson, and J. C. Campbell, "A 130-km transmission experiment at 2 Gbit/s using silica-core fiber and a vapor phase transported DFB laser," presented by ECOC, Stuttgart, W. Germany, 1984.
- [9] A. H. Gnauck, B. L. Kasper, R. A. Linke, R. W. Dawson, T. L. Koch, T. J. Bridges, E. G. Burkhardt, R. T. Yen, D. P. Wilt, J. C. Campbell, K. Ciemiecki Nelson, and L. G. Cohen, "4-Gbit/s transmission over 103 km of optical fiber using a novel electronic multiplexer/demultiplexer," *J. Lightwave Technol.*, vol. LT-3, pp. 1032-1035, Oct. 1985.
- [10] G. P. Agrawal and T. M. Shen, "Effect of fiber-far-end reflections on the bit error rate in optical communications with single-frequency semiconductor lasers," *J. Lightwave Technol.*, vol. LT-4, pp. 58-63, Jan. 1986.
- [11] M. Kitamura, M. Seki, M. Yamaguchi, I. Mito, Ke. Kobayashi and Ko. Kobayashi, "High-power single-longitudinal-mode operation of 1.3- μm DFB-DC-PBH LD," *Electron. Lett.*, vol. 19, pp. 840-841, Sept. 1983.
- [12] D. P. Wilt, R. Yen, T. Wessel, P. Besomi, R. L. Brown, T. Cella, N. K. Dutta, and P. J. Anthony, "Single longitudinal mode distributed feedback double channel planar buriheterostructure 1.55- μm in InGaAsP/InP lasers," presented at IEDM, San Francisco, CA, Dec. 1984.
- [13] C. H. Henry, P. S. Henry, and M. Lax, "Partition fluctuations in nearly single-longitudinal-mode lasers," *J. Lightwave Technol.*, vol. LT-2, pp. 209-216, 1984.
- [14] T. M. Shen and G. P. Agrawal, "Theoretical analysis of mode partition noise in single-frequency semiconductor lasers," *Electron. Lett.*, vol. 21, pp. 1220-1221, Nov. 1985.
- [15] R. A. Linke, B. L. Kasper, C. A. Burrus, I. P. Kaminow, J. S. Ko, and T. P. Lee, "Mode power partition events in nearly single-frequency lasers," *J. Lightwave Technol.*, vol. LT-3, pp. 706-712, June 1985.
- [16] J. C. Campbell, A. G. Dentai, W. S. Holden, and B. L. Kasper, "High-performance avalanche photodiode with separate absorption 'grading' and multiplication regions," *Electron. Lett.*, vol. 19, pp. 818-819, Sept. 1983.
- [17] R. G. Smith and S. D. Personick, in *Semiconductor Devices for Optical Communication*, H. Kressel, Ed. Berlin, W. Germany: Springer-Verlag, 1982, ch. 4, pp. 89-160.
- [18] D. Gloge, A. Albanese, C. A. Burrus, E. L. Chinnock, J. A. Copeland, A. G. Dentai, T. P. Lee, Tingye Li and K. Ogawa, "High-

speed digital lightwave communication using LED's and p-i-n photodiodes at 1.3 μm ," *Bell Syst. Tech. J.*, vol. 59, pp. 1365-1383, Oct. 1980.

- [19] A. B. Sharma, S. J. Holme, and M. M. Butusov, *Optical Fiber Systems and Their Components*. Berlin, W. Germany: Springer-Verlag, 1981, ch. 4, pp. 108-151.
- [20] R. J. McIntyre, "Multiplication noise in uniform avalanche diodes," *IEEE Trans. Electron. Lett.*, vol. ED-13, pp. 164-168, Jan. 1966.
- [21] D. Marcuse, "Computer simulation of laser photon fluctuations: Theory of single-cavity laser," *IEEE J. Quantum Electron.*, vol. QE-20, pp. 1139-1147, Oct. 1984.
- [22] S. E. Miller and D. Marcuse, "On fluctuations and transients in injection lasers," *IEEE J. Quantum Electron.*, vol. QE-20, pp. 1032-1044, Sept. 1984.
- [23] B. L. Kasper, J. C. Campbell, and A. G. Dentai, "Measurements of the statistics of excess noise in separate absorption, grading, and multiplication (SAGM) avalanche photodiodes," *Electron. Lett.*, vol. 20, pp. 796-798, Sept. 1984.

*



Tek-Ming Shen (M'81) was born in Hong Kong on January 6, 1949. He received the B.Sc. degree with highest honors in physics and mathematics, the B.Sc. (special) honors degree in physics from the University of Hong Kong, in 1972 and 1973, respectively, and the Ph.D. degree in physics from the University of California, Berkeley, in 1979.

From 1979 to 1980 he was a Postdoctoral Research Physicist at the University of California, Berkeley. During his doctoral and postdoctoral work, he researched on superconductor-insulator-superconductor tunnel junctions as millimeter-wave mixers. In 1980 he joined the Technical Staff of AT&T Bell Laboratories, Murray Hill, NJ, where he has been involved in the characterization of dynamic properties InGaAsP multifrequency and single-frequency semiconductor lasers and their performance in lightwave communication systems.

*



Govind P. Agrawal (M'83-SM'86) was born in Kashipur, India, on July 24, 1951. He received the M.S. and Ph.D. degrees in physics from the Indian Institute of Technology, New Delhi, India, in 1971 and 1974, respectively.

After spending several years at the Ecole Polytechnique, France, the City University of New York, New York, and Quantel, France, he joined AT&T Bell Laboratories in 1982 as a Member of the Technical Staff. His research interests have been in the fields of quantum electronics, nonlinear

optics, and laser physics. He is an author or coauthor of more than 100 research papers and a book entitled *Long-Wavelength Semiconductor Lasers*. Currently he is engaged in the research and development of semiconductor lasers.

Dr. Agrawal is a member of the American Physical Society and a fellow of the Optical Society of America.